

## Article

# Probabilistic Power Flow Method Considering Continuous and Discrete Variables

Xuexia Zhang \*, Zhiqi Guo and Weirong Chen

School of Electrical Engineering, Southwest Jiaotong University, Chengdu 610031, China;  
guoguo@my.swjtu.edu.cn (Z.G.); wrchen@swjtu.edu.cn (W.C.)

\* Correspondence: survival\_zxx@sina.com; Tel.: +86-28-8760-3332

Academic Editor: William Holderbaum

Received: 26 March 2017; Accepted: 19 April 2017; Published: 26 April 2017

**Abstract:** This paper proposes a probabilistic power flow (PPF) method considering continuous and discrete variables (continuous and discrete power flow, CDPF) for power systems. The proposed method—based on the cumulant method (CM) and multiple deterministic power flow (MDPF) calculations—can deal with continuous variables such as wind power generation (WPG) and loads, and discrete variables such as fuel cell generation (FCG). In this paper, continuous variables follow a normal distribution (loads) or a non-normal distribution (WPG), and discrete variables follow a binomial distribution (FCG). Through testing on IEEE 14-bus and IEEE 118-bus power systems, the proposed method (CDPF) has better accuracy compared with the CM, and higher efficiency compared with the Monte Carlo simulation method (MCSM).

**Keywords:** probabilistic power flow (PPF); discrete variable; cumulant method (CM); deterministic power flow (DPF) calculation

## 1. Introduction

Probabilistic power flow (PPF) was first proposed by Borkowska in 1974 [1], and is an effective probabilistic analysis method for the exploration of the influence of stochastic factors on power systems [2]. Stochastic factors such as loads, wind power generations (WPGs), and fuel cell generations (FCGs) exist widely in practical power systems [3]. Deterministic power flow (DPF) calculations cannot comprehensively evaluate the effects on power systems because of various stochastic factors. However, PPF can completely investigate various stochastic factors and obtain probability distributions of power flow responses (bus voltages and branch power flows), such as probability density functions (PDFs) and cumulative density functions (CDFs) [4]. Therefore, calculation results achieved by the PPF method can better reflect the operating characteristics of power systems.

PPF methods mainly include three categories: simulation methods [5–7], approximate methods [8–11], and analytical methods [12–16]. Among simulation methods, the Monte Carlo simulation method (MCSM) is an outstanding representation, and it is regarded as a standard to evaluate the accuracy and efficiency of other PPF methods. However, MCSM requires tens of thousands of DPF calculations to converge. This computational burden greatly reduces MCSM's efficiency [17].

To improve the computational speed of MCSM, a point estimate method (PEM) is proposed, which is a classical approximate method. Nevertheless, probability distributions of power flow responses cannot be attained accurately because large errors of high order moments are unavoidable [18].

To obtain the probability distributions of power flow responses accurately and reduce errors from PEM, cumulant method (CM) is presented, which is an analytical method. PDFs and CDFs of power flow responses can be obtained by CM accurately and efficiently for PPF problems [19,20]. Nonetheless, errors based on CM still exist, and mainly consist of two classes: (1) linearization errors—when non-linear power flow equations are linearized into linear power flow equations by

ignoring high-order terms of Taylor series expression, linearization errors are formed [21]; and (2) series expansion errors—when series diverge, such as the Gram-Charlier series (GCS) [22], PDFs will appear negative or CDFs will be more than 1 [14]. In a word, two types of errors are mainly derived from the fluctuation of stochastic variables. The larger the fluctuation range of stochastic variables is, the larger the errors are.

To reduce errors in CM, many research achievements have been developed. Hong et al. [23] focus on decreasing linearization errors when the sensitivity matrix of PPF is singular. However, only continuous variables are considered in this paper. Sanabria & Dillon [24] and Hu & Wang [25] present the von Mises method to deal with discrete variables. However, probability distributions of power flow responses cannot be obtained accurately, because the von Mises method handles discrete variables with an approximate approach. Leite da Silva and Arienti [26] used multiple points of linearization to decrease errors from linear power flow equations considering only continuous variables. Meanwhile, searching linearization points is a challenge. Li et al. [27] adopt the same algorithm from [26], considering discrete and continuous variables. Wu et al. [28] present a multiple integral method based on CM to reduce the calculation burden and improve the computational accuracy. However, the number of input random variables is limited, as well as discrete variables that are not involved in this paper. Cai et al. [29] applied MCSM to calculate the cumulants of random input variables with complex probability distributions, but this method cannot diminish errors in CM. When the number of discrete variables increases, the fluctuation range of input random variables will be extended.

In existing studies, FCG and branch outages are two typical discrete variables [25,30]. With FCG becoming a prospective generator as a discrete variable, that discrete variable causes the fluctuation range of random input variables larger in CM to become a notable issue. Furthermore, continuous and discrete variables are seldom considered simultaneously, and cannot be addressed accurately based only on CM. As a result, it is a challenge for CM to solve these problems [31].

In order to solve PPF problems with continuous and discrete variables accurately, this paper presents a novel PPF method considering continuous and discrete variables (CDPF). In CDPF, CM is employed to handle continuous variables and multiple DPF (MDPF) calculations are presented to deal with discrete variables. Then, probability distributions of power flow responses can be calculated accurately and efficiently by the convolution of continuous and discrete variables of power flow responses. The main contributions of this paper include following aspects:

- (1) This paper proposes a novel PPF method (CDPF) that can accurately solve PPF problems with continuous and discrete variables simultaneously. In CDPF, multiple probability distributions of continuous variables and discrete variables can be considered together, such as normal distribution (loads), non-normal distribution (WPGs), and binomial distribution (FCGs).
- (2) This paper investigates two issues affecting power systems: (1) What are effects of a discrete variable (FCG) under different rated powers on power systems in Case 2, Section 4; and (2) How can we address multiple discrete variables (FCGs) in power systems in Case 3, Section 4?
- (3) The accuracy and efficiency of CDPF are verified quite well compared with results of bus voltages and branch power flows obtained by CDPF, CM, and MCSM in IEEE 14-bus and IEEE 118-bus power systems.

The main framework of this paper is organized as follows: Section 2 introduces probability distributions of WPGs, FCGs, and loads which are used in this paper; Section 3 describes the CDPF method in detail; Section 4 shows case studies and analysis results; and Section 5 draws conclusions.

## 2. Probability Distributions of Generations and Loads

In this paper, continuous and discrete variables are considered simultaneously, in which the output power of WPGs and loads are regarded as continuous variables, and the output power of FCGs

are regarded as discrete variables. This section shows probability distributions of generations and loads in power systems. The details are described below.

### 2.1. The Output Power PDF of WPGs

The active output power PDF of WPGs can be described as follows [5]:

$$f(P_{WPG}) = \begin{cases} 1 - \exp\left[-\left(\frac{v_{ci}}{c}\right)^k\right] + \exp\left[-\left(\frac{v_{co}}{c}\right)^k\right] & P_{WPG} = 0 \\ \frac{k}{k_1 c} \left(\frac{P_{WPG} - k_2}{k_1 c}\right)^{k-1} \exp\left[-\left(\frac{P_{WPG} - k_2}{k_1 c}\right)^k\right] & 0 < P_{WPG} < P_{WPGR} \\ \exp\left[-\left(\frac{v_r}{c}\right)^k\right] - \exp\left[-\left(\frac{v_{co}}{c}\right)^k\right] & P_{WPG} = P_{WPGR} \end{cases} \quad (1)$$

where  $v_{ci}$ ,  $v_r$ , and  $v_{co}$  are, respectively, the cut-in wind speed, the rated wind speed, and the cut-out wind speed of WPGs.  $v$  is the wind speed,  $k$  is a shape parameter, and  $c$  is a scale parameter.  $k$  and  $c$  can be calculated by the mean value and standard deviation of the wind speed obtained from the historical wind speed data.  $P_{WPGR}$  is the rated power of WPGs.  $k_1 = P_{WPGR}/(v_r - v_{ci})$  and  $k_2 = -k_1 \times v_{ci}$ .

In this paper, the wind speed model follows a two-parameter Weibull distribution [5], and buses connected with WPGs are set to PQ buses. The reactive power  $Q_{WPG}$  can be obtained according to the active power  $P_{WPG}$  and the constant power factor.

### 2.2. The Active and Reactive Power PDF of Loads

The active and reactive power PDF of loads follow a normal distribution [21], shown as follows:

$$f(P_L) = \frac{1}{\sqrt{2\pi}\sigma_{P_L}} \exp\left[-\frac{(P_L - \mu_{P_L})^2}{2\sigma_{P_L}^2}\right] \quad (2)$$

$$f(Q_L) = \frac{1}{\sqrt{2\pi}\sigma_{Q_L}} \exp\left[-\frac{(Q_L - \mu_{Q_L})^2}{2\sigma_{Q_L}^2}\right] \quad (3)$$

where  $P_L$  and  $Q_L$  are, respectively, the active and reactive power of loads;  $\mu_{P_L}$  and  $\sigma_{P_L}$  are, respectively, the mean value and standard deviation of the active power;  $\mu_{Q_L}$  and  $\sigma_{Q_L}$  are, respectively, the mean value and standard deviation of the reactive power.

### 2.3. The Output Power Probability Distribution of FCGs

The status of single FCGs include the operation and shutdown [32]. Therefore, the active output power of multiple FCGs is usually assumed to follow a binomial distribution, listed as follows:

$$P_{FCG,i} = C_n^i (1 - sd)^i sd^{n-i} \quad (4)$$

$$x_i = s \cdot i \quad (5)$$

where  $n$  is the total number of FCGs,  $i$  is the number of FCGs which are in the operational status,  $sd$  is the probability value of a single FCG in the shutdown status,  $s$  is the rated power of a single FCG.  $P_{FC,i}$  is the probability value when the number of FCGs in the operation status is  $i$ .  $x_i$  is the total active power of FCGs in the operation status. Buses connected with FCGs are set to PQ buses with a constant power factor. Probability distributions of the reactive power can be obtained according to the probability distributions of the active power and power factors.

## 3. CDPF Method

In CDPF, PDFs of power flow responses considering continuous variables ( $P_{WPG}$ ,  $Q_{WPG}$ ,  $P_L$ ,  $Q_L$ ) can be obtained by CM. Then, probability distributions of the power flow responses that consider the

discrete variables ( $P_{FCG}$ ,  $Q_{FCG}$ ) can be accurately calculated by MDPF calculations. Moreover, PDFs of power flow responses considering all of the variables can be achieved accurately and efficiently by the convolution of the above two results (CM and MDPF). In this section, fundamental theories, concepts, and implementations of CDPF are stated in detail.

### 3.1. Power Flow Responses with Continuous Variables Based on CM

#### 3.1.1. Calculation on Continuous Variable Cumulants

In CM, cumulants of continuous variables are calculated based on an analytical method. The  $\gamma$  order moment of continuous variable  $x$  is defined as follows [33]:

$$\alpha_\gamma = \int_{-\infty}^{+\infty} x^\gamma f(x) dx \quad (6)$$

where  $\gamma$  is the order number of moments and  $f(x)$  is the PDF of  $x$ , where  $x$  is the  $P_{WPG}$  (or  $Q_{WPG}$ ,  $P_L$ ,  $Q_L$ ) in this paper.

The relationship between the  $\gamma$  order cumulant  $k_\gamma$  and the moments can be described as follows [33]:

$$k_\gamma = \begin{cases} \alpha_1 & \gamma = 1 \\ \alpha_\gamma - \sum_{j=1}^{\gamma-1} C_{\gamma-1}^j \alpha_j k_{\gamma-j} & \gamma > 1 \end{cases} \quad (7)$$

#### 3.1.2. Linear Power Flow Equations

Nonlinear power flow equations can be written as follows [34]:

$$\begin{cases} \mathbf{W} = f(\mathbf{X}) \\ \mathbf{Z} = g(\mathbf{X}) \end{cases} \quad (8)$$

where  $\mathbf{W}$  is the vector composed of the active and reactive power from generations and loads.  $\mathbf{X}$  is the vector composed of voltage amplitudes and voltage phase angles at all buses.  $\mathbf{Z}$  is the vector composed of the active and reactive power of branch power flows.  $f(x)$  and  $g(x)$  are, respectively, functions of the bus voltage and branch power flow.

Equation (8) is linearized into Equation (9) at  $\mathbf{X}_0$  and  $\mathbf{Z}_0$ . Linear power flow equations are as follows [34]:

$$\begin{cases} \mathbf{X} = \mathbf{X}_0 + \mathbf{J}_0^{-1} \Delta \mathbf{W} \\ \mathbf{Z} = \mathbf{Z}_0 + \mathbf{G}_0 \mathbf{J}_0^{-1} \Delta \mathbf{W} \end{cases} \quad \mathbf{G}_0 = \left. \frac{\partial \mathbf{Z}}{\partial \mathbf{X}} \right|_{\mathbf{X}=\mathbf{X}_0} \quad (9)$$

where  $\mathbf{X}_0$  and  $\mathbf{Z}_0$  are, respectively, mean vectors of bus voltages and branch power flows,  $\mathbf{J}_0$  is the Jacobi matrix obtained by DPF calculation in the maximal iteration,  $\Delta \mathbf{W}$  is each order cumulant vector composed of the active and reactive power from generations and loads, and  $\mathbf{G}_0$  is the sensitivity matrix of the branch power flow function  $g(x)$ .

According to Equation (9), each order cumulant vector of  $\mathbf{X}$  and  $\mathbf{Z}$  can be obtained efficiently.

#### 3.1.3. Estimation on Probability Distributions of Power Flow Responses

According to each order cumulant vector of  $\mathbf{X}$  and  $\mathbf{Z}$ , probability distributions of bus voltages and branch power flows can be obtained based on GCS. GCS can be expressed as Equation (10) [35]:

$$f_X(x) = f_0(x) \left[ 1 + \sum_{i=1}^{+\infty} \lambda_i H_i \right] \quad (10)$$

where  $f_X(x)$  is the PDF of the power flow response,  $f_0(x)$  is the PDF of the standard normal distribution,  $\lambda_i$  is the coefficient of series expansion, and  $H_i$  is the  $i$ th order Hermite orthogonal polynomial.

### 3.2. Power Flow Responses with Discrete Variables Based on MDPF Calculations

#### 3.2.1. Determination on the Vector of Discrete Variables

Suppose that  $n$  FCGs are regarded as  $n$  discrete variables  $X_i$  (where  $i \in \{1, 2, \dots, n\}$ ) in a power system. The vector  $\mathbf{X}$  of discrete variables is defined as follows:

$$\mathbf{X} = [X_1, X_2, \dots, X_i, \dots, X_n] \quad (11)$$

where  $\mathbf{X}$  denotes the output power vector of FCGs.  $X_i$  can be expressed as follows:

$$X_i \in (x_{j_1}, x_{j_2}, \dots, x_{j_i}, \dots, x_{j_n}), 1 \leq j_i \leq J_i, i \in \{1, 2, \dots, n\} \quad (12)$$

where the number of work statuses on the  $i$ th FCG  $X_i$  is  $J_i$ , and  $x_{j_i}$  is the output power of the  $i$ th FCG  $X_i$  at the  $j_i$  work status.

The probability distribution of  $X_i$  can be shown as follows:

$$p_{j_i} = P_i(X_i = x_{j_i}), i \in \{1, 2, \dots, n\} \quad (13)$$

where  $p_{j_i}$  is the probability value of  $X_i = x_{j_i}$  when the  $i$ th fuel cell  $X_i$  works at  $j_i$  status.  $P_i$  is the probability distribution.

Supposing that  $n$  discrete variables  $[X_1, X_2, \dots, X_i, \dots, X_n]$  are independent of each other, the probability distribution of  $\mathbf{X}$  can be denoted as Equation (14):

$$P_1(X_1 = x_{j_1}) \cdot P_2(X_2 = x_{j_2}) \cdot \dots \cdot P_i(X_i = x_{j_i}) \cdot \dots \cdot P_n(X_n = x_{j_n}) = p_{j_1} \cdot p_{j_2} \cdot \dots \cdot p_{j_i} \cdot \dots \cdot p_{j_n} \quad (14)$$

#### 3.2.2. Determination on the Active Power and Reactive Power Vector of Generations and Loads

Input vectors in MDPF calculations include the active power and reactive power of continuous and discrete variables. For continuous variables, input values of the active power and reactive power are corresponding mean values of WPGs, and the loads are stated as  $E_{c1}, E_{c2}, \dots, E_{cm}$ . Subscripts  $c_1, c_2, \dots, c_m$  are numbers of injection buses.  $m$  is the number of continuous variables.

For discrete variables, values of the active power and reactive power of FCGs can be described as follows:

$$X_i = (x_{j_i}), i \in \{1, 2, \dots, n\} \quad (15)$$

Input vectors in the MDPF calculation can be described as follows:

$$\mathbf{A}_k = [0, 0, \dots, 0, E_{c1}, \dots, E_{c2}, \dots, E_{cm}, \dots, x_{j_1}, x_{j_2}, \dots, x_{j_i}, \dots, x_{j_n}]_N, 1 \leq k \leq J_1 \cdot J_2 \cdot \dots \cdot J_n \quad (16)$$

where  $k$  is from 1 to  $J_1 \cdot J_2 \cdot \dots \cdot J_n$ . The dimension of  $\mathbf{A}_k$  is  $N$  which is the number of buses of the power system. Note that "0" elements in  $\mathbf{A}_k$  denote no input power or output power.

#### 3.2.3. Calculations Based on MDPF

Take  $\mathbf{A}_k$  of Equation (16) as the  $k$ th active power and reactive power vector  $\mathbf{W}_k$  in Equation (8); then, power flow responses (bus voltages and branch power flows) can be obtained using  $\mathbf{W}_k$  based on the DPF calculation. The bus voltage vectors can be described as follows:

$$\mathbf{B}_k = [U_1, U_2, \dots, U_N]_N, 1 \leq k \leq J_1 \cdot J_2 \cdot \dots \cdot J_n \quad (17)$$

where  $U_1, U_2, \dots, U_N$  are, respectively, bus voltages of bus-1, bus-2,  $\dots$ , bus- $N$ , and  $N$  is the bus number of the power system.

Using the same method, vectors of branch power flows  $\mathbf{C}_k$  also can be obtained, and numbers of  $\mathbf{B}$  and  $\mathbf{C}$  are both  $J_1 \cdot J_2 \cdot \dots \cdot J_n$ .

### 3.3. Convolution of Continuous and Discrete Variables

When multiple input random variables ( $\Delta \mathbf{W}_{c1}, \dots, \Delta \mathbf{W}_{cm}, \Delta \mathbf{W}_{d1}, \dots, \Delta \mathbf{W}_{dn}$ ) exist in the power system, Equation (9) can be further expressed as follows:

$$\mathbf{X} = \mathbf{X}_0 + \mathbf{J}_0^{-1}(\Delta \mathbf{W}_{c1} * \dots * \Delta \mathbf{W}_{cm} * \Delta \mathbf{W}_{d1} * \dots * \Delta \mathbf{W}_{dn}) \quad (18)$$

$$\mathbf{Z} = \mathbf{Z}_0 + \mathbf{G}_0 \mathbf{J}_0^{-1}(\Delta \mathbf{W}_{c1} * \dots * \Delta \mathbf{W}_{cm} * \Delta \mathbf{W}_{d1} * \dots * \Delta \mathbf{W}_{dn}) \quad (19)$$

However, if all input random variables are convoluted by Equations (18) and (19), the computation efficiency of CDPF will decrease. Considering the accuracy and efficiency of the PPF calculation, random input variables of power systems are only divided into two categories: continuous and discrete random variables, in this paper. Therefore, Equations (18) and (19) can be stated as follows:

$$\begin{cases} \mathbf{X} = \mathbf{X}_0 + \mathbf{J}_0^{-1}(\Delta \mathbf{W}_c * \Delta \mathbf{W}_d) \\ \mathbf{Z} = \mathbf{Z}_0 + \mathbf{G}_0 \mathbf{J}_0^{-1}(\Delta \mathbf{W}_c * \Delta \mathbf{W}_d) \end{cases} \quad (20)$$

where  $\Delta \mathbf{W}_c$  and  $\Delta \mathbf{W}_d$  are, respectively, continuous and discrete vectors, and “\*” is the convolution operator of multiple random variables.

According to Equation (20), results  $\mathbf{X}$  and  $\mathbf{Z}$  of PPF can be efficiently and accurately obtained by the convolution of continuous and discrete variables.

The convolution operation of continuous and discrete variables can be described as follows:

$$Y = C_W * D_W \quad (21)$$

where  $Y$  is the random variable that needs to be obtained,  $C_W$  and  $D_W$  are, respectively, continuous and discrete variables.

PDF and CDF of  $Y$  are defined as follows [25]:

$$f_Y(x) = \sum_{i=1}^n p_i \cdot f_{C_W}(x - x_i) \quad (22)$$

$$F_Y(x) = \sum_{i=1}^n p_i \cdot \int_{-\infty}^x f_{C_W}(x - x_i) dx \quad (23)$$

where  $f_Y(x)$  and  $F_Y(x)$  are, respectively, PDF and CDF of  $Y$ .  $n$  is the number of discrete points of  $D_W$ ,  $x_i$  and  $p_i$  are, respectively, the discrete point value and the probability value of  $D_W$ , and  $f_{C_W}$  is the PDF of  $C_W$ .

### 3.4. Implementation Procedure of CDPF

Based on the above three Sections 3.1–3.3, the complete process of CDPF for PPF problems can be expressed as follows:

Step (1) Set the system parameters of the power system, probability distribution parameters, and bus numbers of input random variables including WPGs, loads, and FCGs.

Step (2) Carry out a DPF calculation to obtain  $\mathbf{X}_0$ ,  $\mathbf{Z}_0$ ,  $\mathbf{J}_0$ , and  $\mathbf{G}_0$  using  $\mathbf{W}_0$ .

Step (3) Obtain each order moment  $\alpha_\gamma$  of the continuous variables by using Equation (6).

Step (4) Calculate each order cumulant  $k_\gamma$  of the continuous variables by using Equation (7), based on the moment  $\alpha_\gamma$  obtained by Step 3.

Step (5) Calculate each order cumulant of the power flow responses  $\mathbf{X}$  and  $\mathbf{Z}$  according to Equation (9).

Step (6) Obtain the PDF based on each order cumulant of the power flow responses according to Equation (10) and then integrate the PDF to acquire the CDF.

Step (7) Determine the vector of discrete input variables according to Equations (11) and (12). Then, calculate the probability distribution of discrete vector according to Equations (13) and (14).

Step (8) Generate input vectors  $\mathbf{A}_k$  of the random active and reactive power variables and the probability value  $P_k$  of  $\mathbf{A}_k$  according to Equations (16) and (14).

Step (9) Carry out MDPF calculations to obtain the output vectors  $\mathbf{B}_k$  and  $\mathbf{C}_k$  of the power flow responses using  $\mathbf{A}_k$ , and the probability value of each  $\mathbf{B}_k$  or  $\mathbf{C}_k$  is  $P_k$  according to Equations (8) and (14).

Step (10) Convolute continuous and discrete variables of power flow responses obtained, respectively, from Step 6 and Step 9 according to Equations (22) and (23). Convolution results are power flow responses considering all continuous and discrete variables. Figure 1 is the flowchart of the power flow considering continuous and discrete variables (CDPF) method.

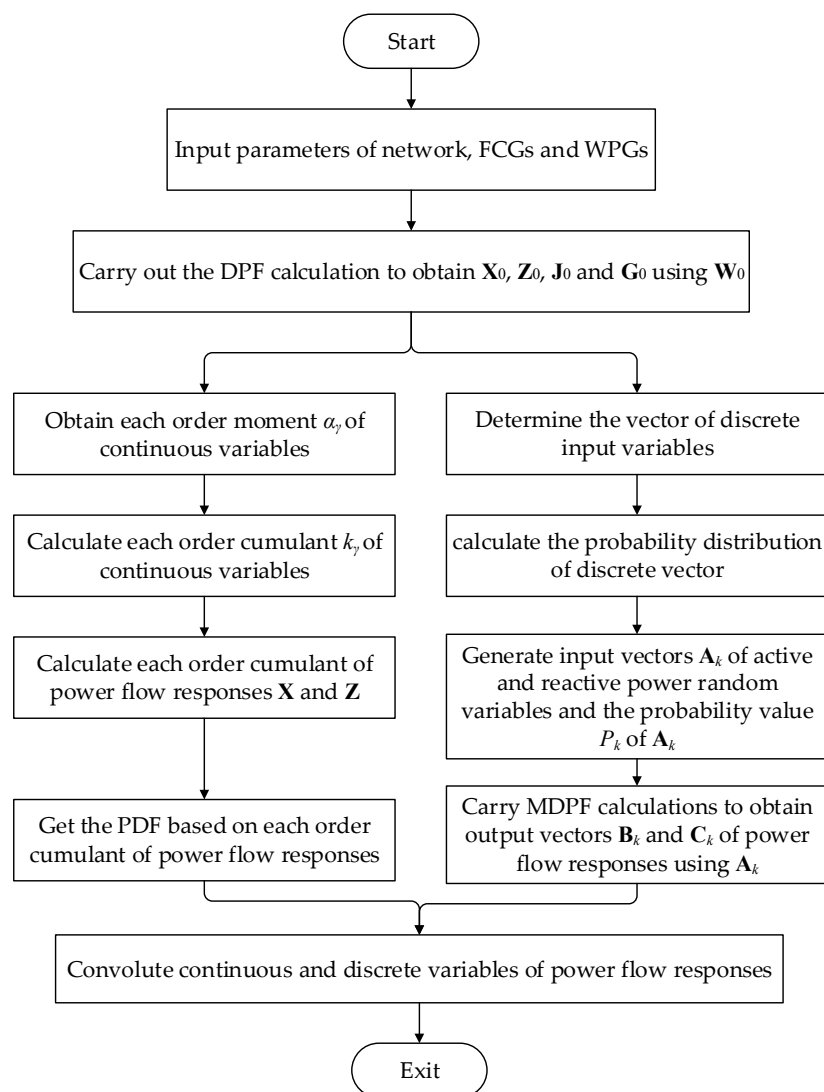


**Figure 1.** Flowchart of the power flow considering continuous and discrete variables (CDPF) method. DPF: deterministic power flow; FCG: fuel cell generator; PDF: probability density function; MDPF: multiple DPF; WPG: wind power generator.

#### 4. Case Studies

The accuracy, efficiency, and applicability of CDPF are verified in this section, including four parts: (1) The CDPF, MCSM, and CM are used to solve PPF problems in an IEEE 14-bus power system. Compared with CM, CDPF has better accuracy; and compared with MCSM, CDPF has higher



efficiency; (2) PPF problems on a FCG under different rated powers are studied to further demonstrate the applicability of CDPF in an IEEE 14-bus power system; (3) the case of multiple FCGs in a power system is considered to demonstrate the applicability of CDPF in an IEEE 14-bus power system; and (4) an IEEE bus-118 power system is applied to verify the performance of CDPF.

#### 4.1. Verification of CDPF by Comparison with MCSM and CM in Accuracy and Efficiency

An IEEE 14-bus power system is used in this part, consisting of 14 buses and 20 branches. Figure 2 is the IEEE 14-bus power system. The loads are supposed to follow a normal distribution, in which mean values are the power value of loads, and standard deviations are 5% of mean values. A WPG with a capability of 10 MW is connected to bus-13, and the constant power control method is adopted in WPG with the power factor  $\cos(\phi) = -0.98$ , the cut-in wind speed of WPG is  $v_{ci} = 3$  m/s, the rated wind speed of WPG is  $v_r = 15$  m/s, and the cut-out wind speed of WPG is  $v_{co} = 25$  m/s. The wind speed model is assumed to follow a two-parameter Weibull distribution with a shape parameter  $k = 2.80$  and a scale parameter  $c = 5.14$ . Two FCGs are connected to bus-13 and bus-14, where each capability of FCG is 20 MW, the power factor  $\cos(\phi) = 0.8$ , and the outage probability is 0.08. DPF calculation times based on MCSM are 10,000, and MCSM is taken as a comparison standard of PPF solutions in this paper.

PDFs of the voltage magnitude of bus-14 gained by the three methods, respectively, are shown in Figure 3. PDF curves of CDPF are almost the same as the ones obtained by MCMS. However, results obtained by CM have a large difference compared with results obtained by MCMS, and negative probability values occur in Figure 3 by CM.

Figures 4 and 5 are CDFs of the active and reactive power, respectively, at branch 20 (from bus-13 to bus-14). In Figures 4 and 5, some values in the CDF curves of CM are more than 1, which violates the probability property. The reason is that the large fluctuation range of random input variables causes a large linearization error of power flow equations.

Means and standard deviations of the voltage magnitude (p.u.) and the active power (p.u.) at branches in the IEEE 14-bus power system are shown, respectively, in Tables 1 and 2. The results obtained by CDPF are closer to standard results obtained by MCMS compared with the results obtained by CM.

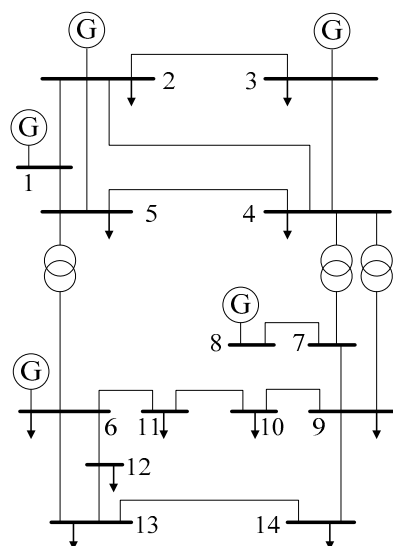
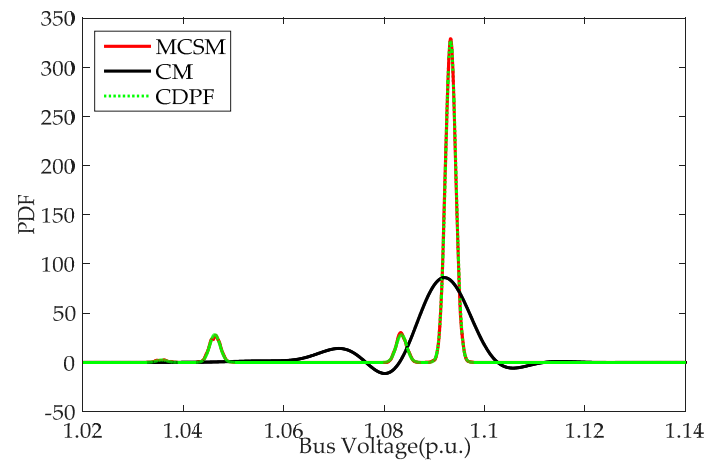
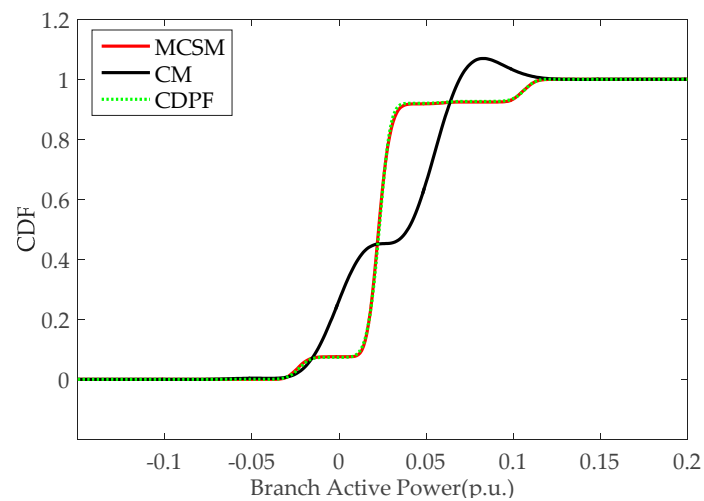


Figure 2. IEEE 14-bus power system.





**Figure 3.** The probability density function (PDF) of the voltage magnitude at bus-14 in an IEEE 14-bus power system. CM: cumulant method; MCSM: Monte Carlo simulation method.



**Figure 4.** The cumulative density function (CDF) of the active power at branch 20 (13–14) in an IEEE 14-bus power system.

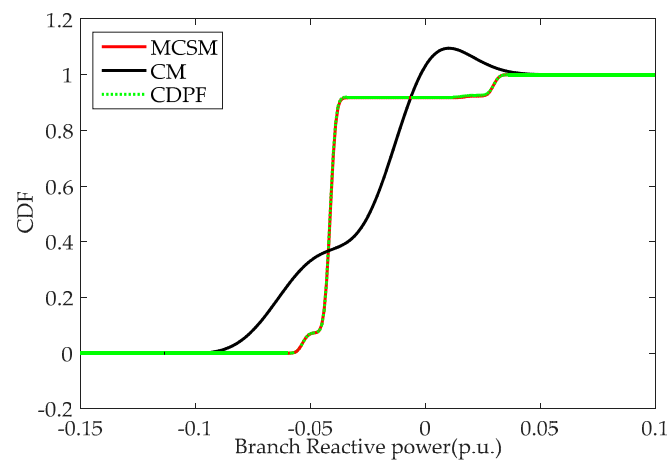


**Figure 5.** The CDF of the reactive power at branch 20 (13–14) in an IEEE 14-bus power system.

**Table 1.** The means and standard deviations of the voltage magnitude (p.u.) in an IEEE 14-bus power system.

Bus No.	Mean Values			Standard Deviation Values		
	MCSM	CM	CDPF	MCSM	CM	CDPF
1	1.0600	1.0600	1.0600	0.0000	0.0000	0.0000
2	1.0450	1.0450	1.0450	0.0000	0.0000	0.0000
3	1.0100	1.0100	1.0100	0.0000	0.0000	0.0000
4	1.0250	1.0251	1.0250	0.0016	0.0012	0.0016
5	1.0266	1.0267	1.0266	0.0015	0.0012	0.0015
6	1.0700	1.0700	1.0700	0.0000	0.0000	0.0000
7	1.0699	1.0700	1.0699	0.0021	0.0016	0.0021
8	1.0900	1.0900	1.0900	0.0000	0.0000	0.0000
9	1.0693	1.0624	1.0693	0.0036	0.0030	0.0036
10	1.0619	1.0620	1.0619	0.0030	0.0025	0.0030
11	1.0624	1.0624	1.0624	0.0016	0.0013	0.0016
12	1.0690	1.0690	1.0690	0.0030	0.0028	0.0030
13	1.0808	1.0809	1.0809	0.0066	0.0055	0.0065
14	1.0886	1.0889	1.0887	0.0131	0.0094	0.0131

**Table 2.** The means and standard deviations of the active power (p.u.) at the branches in an IEEE 14-bus power system.

Bus No.	Mean Values			Standard Deviation Values		
	MCSM	CM	CDPF	MCSM	CM	CDPF
1	1.2985	1.2982	1.2987	0.0709	0.0708	0.0712
2	0.6044	0.6043	0.6046	0.0349	0.0350	0.0352
3	0.6790	0.6790	0.6791	0.0299	0.0299	0.0300
4	0.4572	0.4571	0.4572	0.0239	0.0242	0.0241
5	0.3160	0.3159	0.3161	0.0211	0.0211	0.0213
6	0.2829	0.2831	0.2830	0.0238	0.0238	0.0239
7	0.5917	0.5917	0.5917	0.0204	0.0211	0.0205
8	0.1723	0.1723	0.1724	0.0235	0.0246	0.0237
9	0.0990	0.0990	0.0991	0.0134	0.0141	0.0135
10	0.2250	0.2249	0.2253	0.0441	0.0430	0.0446
11	0.0902	0.0902	0.0902	0.0088	0.0089	0.0090
12	0.0251	0.0251	0.0252	0.0111	0.0101	0.0113
13	0.0023	0.0024	0.0021	0.0375	0.0391	0.0380
14	0.0000	0.0000	0.0000	0.0000	0.0000	0.0000
15	0.1723	0.1723	0.1724	0.0235	0.0246	0.0237
16	0.0359	0.0359	0.0360	0.0092	0.0091	0.0093
17	0.0596	0.0597	0.0595	0.0345	0.0359	0.0348
18	0.0543	0.0543	0.0543	0.0087	0.0086	0.0088
19	0.0360	0.0360	0.0359	0.0110	0.0103	0.0112
20	0.0258	0.0256	0.0258	0.0261	0.0261	0.0263

The CPU time and calculation number  $N_{PL}$  of DPF are shown in the Table 3.  $N_{PL}$  of CDPF includes a DPF calculation based on CM to handle continuous variables and DPF calculations of  $2^n$  times to handle  $n$  discrete variables. The CPU time of CDPF also mainly includes the above two types of calculation times, in which it is the major part for handling discrete variables based on MDPF calculations. Compared with MCSM, the CPU time and  $N_{PL}$  of CDPF can be greatly reduced. To promote calculation accuracy and reduce the CPU time and  $N_{PL}$ , CDPF makes good use of simulation (MDPF) and analytical methods (CM). Compared with CM, the CPU time and  $N_{PL}$  of CDPF are slightly increased because of the cost for enhancing the calculation accuracy.

**Table 3.** CPU time and calculation number  $N_{PL}$  of the DPF.

MCSM		CM		CDPF	
$N_{PL}$	CPU Time (s)	$N_{PL}$	CPU Time (s)	$N_{PL}$	CPU Time (s)
10,000	181.0645	1	0.0800	5	0.3144

Notes:  $N_{PL}$  is the calculation number of the DPF; CPU: Central Processing Unit.

#### 4.2. PPF Analysis on a FCG under Different Rated Powers

To further demonstrate the applicability of CDPF, a test of the accuracy of CDPF is carried out under an FCG with different rated powers. The FCG is only set at bus-14, and rated powers are, respectively, 0 MW, 10 MW, 20 MW, 30 MW and 40 MW. Except for the rated power of FCGs, other parameters of FCGs, positions, and parameters of WPGs are the same as those in Part 1 of Section 4.

The PDFs of the voltage magnitude at bus-14 with the rated power of the FCGs at bus-14 being 0 MW, 10 MW, 20 MW, 30 MW and 40 MW, respectively, are shown in Figure 6 by three methods. The results of CDPF are almost the same as the results of MCSM at different rated powers of the FCGs. Compared with MCSM, the accuracy of CM gradually decreases with the rated power of the FCGs gradually increasing. With the rated power of FCGs increasing, the rate of total active power of FCGs is increased, which increases the fluctuation range of discrete variables. Meanwhile, the linearization errors and the series expansion errors are both increased. Hence, the accuracy of CM decreases and the results verify this conclusion.

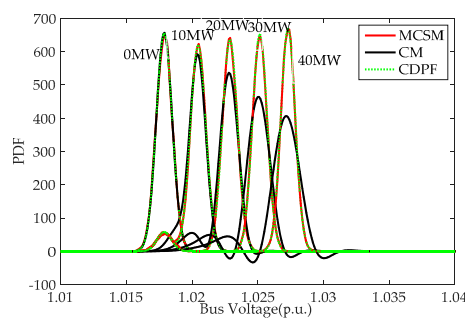


**Figure 6.** The PDFs of the voltage magnitude at bus-14 with the rated power of FCG at bus-14 being 0 MW, 10 MW, 20 MW, 30 MW and 40 MW, respectively, in an IEEE 14-bus power system.

The means and standard deviations of the voltage magnitude at PQ buses with the rated power of FCG at bus-14 being 0 MW, 10 MW, 20 MW, 30 MW and 40 MW, respectively, are shown in Figures 7 and 8 by MCSM and CDPF. The results of CDPF are almost the same as results of MCSM on means and standard deviations of the voltage magnitude at PQ buses.

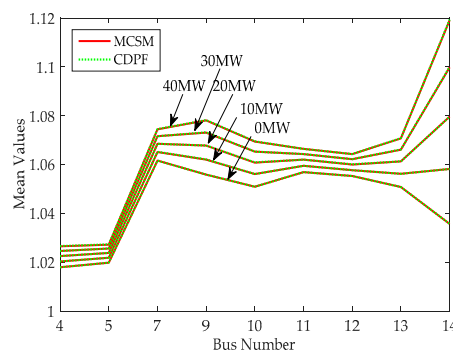


**Figure 7.** The means of the voltage magnitude at PQ buses with the rated power of the FCG at bus-14 being 0 MW, 10 MW, 20 MW, 30 MW and 40 MW, respectively, in an IEEE 14-bus power system.

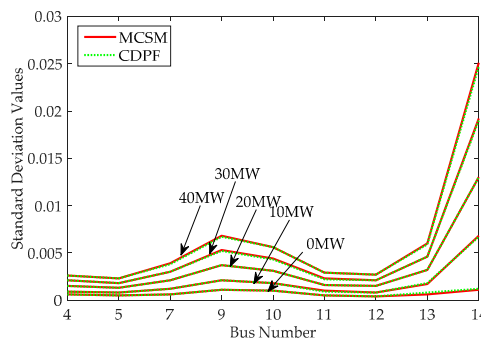


**Figure 8.** The standard deviations of the voltage magnitude at PQ buses with the rated power of the FCG at bus-14 being 0 MW, 10 MW, 20 MW, 30 MW and 40 MW, respectively, in an IEEE 14-bus power system.

#### 4.3. PPF Analysis on Multiple FCGs in an IEEE 14-Bus Power System

To further demonstrate the applicability of CDPF, four cases on the accuracy and efficiency of CDPF are carried when multiple FCGs exist in an IEEE 14-bus power system. In all cases, the total power of FCGs is assumed to be constant, while the number and position of FCGs connected in the power system are alternative. In the first case, the number of FCGs connected in the IEEE 14-bus power system is one and the position of FCG is at bus-14, with the rated power of each FCG being 10 MW. In the second case, the number of FCGs connected in the IEEE 14-bus power system is two and the positions of the FCGs are at bus-13 and bus-14, with the rated power of each FCG being 5 MW. In the third case, the number of FCGs connected in the IEEE 14-bus power system is three, and positions of FCGs are at bus-12, bus-13 and bus-14, with the rated power of each FCG 3.33 MW. In the fourth case, the number of FCGs connected in the IEEE 14-bus power system is five and positions of the FCGs are at bus-10, bus-11, bus-12, bus-13 and bus-14, with the rated power of each FCG being 2 MW. Other settings of parameters, including the power system network, traditional generators, WPG, and loads, are the same as those of Part 1 in Section 4.

PDFs of the voltage magnitude at bus-14 with one, two, three, and five FCGs, respectively, at different buses in the IEEE 14-bus power system are shown in Figure 9 by three methods. The results of CDPF are almost the same as the results of MCSM in different numbers of FCGs, which is to say that solutions obtained by CDPF can match standard solutions obtained by MCSM rather well, yet the accuracy of CM gradually decreases with the number of FCGs increasing compared with MCSM. With the number of FCGs increasing, the linearization errors and the series expansion errors are both increased in CM. Hence, the accuracy of CM decreases and the results verify this conclusion.

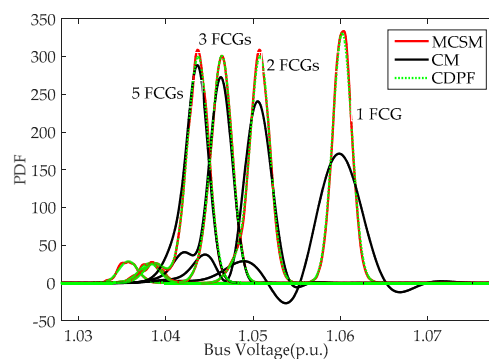


**Figure 9.** The PDFs of the voltage magnitude at bus-14 with one, two, three and five FCGs, respectively, at different buses in an IEEE 14-bus power system.

The means and standard deviations of the voltage magnitude at PQ buses with one, two, three, and five FCGs, respectively, at different buses in the IEEE 14-bus power system are shown in Figures 10 and 11 by MCSM and CDPF. Results obtained by CDPF are almost the same as those obtained by MCSM with respect to means and standard deviations of the bus voltage magnitude at PQ buses.

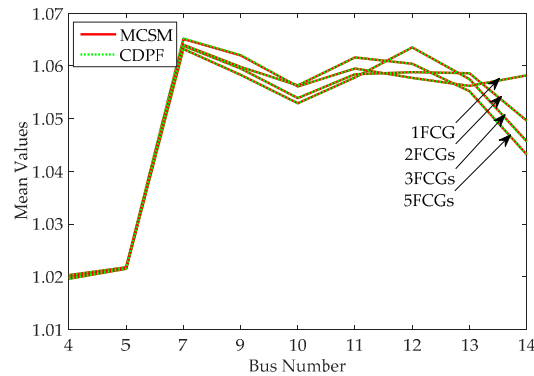


**Figure 10.** The means of the voltage magnitude at PQ buses with one, two, three and five FCGs, respectively, at different buses in an IEEE 14-bus power system.

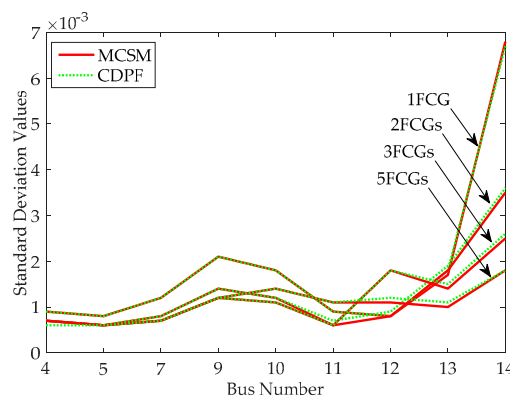


**Figure 11.** Standard deviations of the voltage magnitude at PQ buses with one, two, three and five FCGs, respectively, at different buses in an IEEE 14-bus power system.

CPU time and calculation number  $N_{PL}$  of three methods are shown in Table 4. Compared with MCSM, CDPF requires less CPU time and  $N_{PL}$  for each case. Note that with the number of FCGs increasing, CPU time and  $N_{PL}$  are also increased in CDPF because computation iterations for MDPF are related to the number of FCGs.

**Table 4.** CPU time and calculation number  $N_{PL}$  of DPF.

FCG Number	MCSM		CM		CDPF	
	$N_{PL}$	CPU Time (s)	$N_{PL}$	CPU Time (s)	$N_{PL}$	CPU Time (s)
1	10,000	183.3972	1	0.0623	3	0.1461
2	10,000	180.8913	1	0.0624	5	0.2492
3	10,000	182.4137	1	0.0671	9	0.4970
5	10,000	183.9572	1	0.0661	33	2.0045

#### 4.4. The Test in the IEEE 118-Bus Power System

To demonstrate the applicability of CDPF on large power systems, an IEEE 118-bus power system is used in this part. Details on the IEEE 118-bus power system are: 118 buses; 186 branches; a 500 MW WPG plant is set at bus-2 and nine FCG plants are set, respectively, at bus-3, bus-5, bus-7, bus-9, bus-11,

bus-13, bus-14, bus-16 and bus-17, the rated power of each FCG plant is 200 MW; other settings of WPGs and loads can be referred to those of Part 1 in Section 4. In the IEEE 118-bus power system, 119 continuous input variables (a WPG and 118 loads) and nine discrete input variables (nine FCGs) are considered in this paper.

PDFs of the voltage magnitude at bus-3, bus-57 and bus-118 are shown in Figure 12 by three methods. CDPF and CM perform well with respect to the accuracy of voltage magnitudes at bus-57 and bus-118. Specifically, we can see that PDFs of the voltage magnitude at bus-57 and bus-118 obtained by CDPF are closer to that obtained by MCSM than that by CM. Especially, the accuracy of the voltage magnitude at bus-3 in CDPF is much higher than that in CM. The main reason is that bus-3 is close to WPG, and the FCGs result in a larger impact on bus-3 than on bus-57 and bus-118.

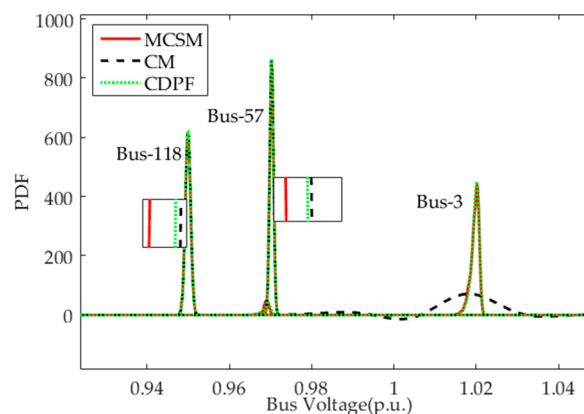


**Figure 12.** The PDFs of the voltage magnitude at bus-3, bus-57 and bus-118 in an IEEE 118-bus power system.

Means and standard deviations of the voltage magnitude at PQ buses in IEEE 118-bus power system are shown in Figures 13 and 14. In general, CDPF and CM can well approach the standard results based on MCSM with respect to mean and standard deviation indices. Specifically, we can see that the green line denoting the CDPF is closer to the red line denoting the MCSM than the black line denoting the CM in Figures 13 and 14. Yet, the standard deviation in the CM has larger errors compared with that in MCSM at some buses in Figure 14.

CPU time and calculation number  $N_{PL}$  of three methods are shown in Table 5. CPU time and  $N_{PL}$  of CDPF are obviously decreased compared with those in MCSM. Although CDPF's CPU time is slightly increased compared with that in CM, CDPF can still inherit MCSM's computational accuracy advantage and CM's computational speed merit.

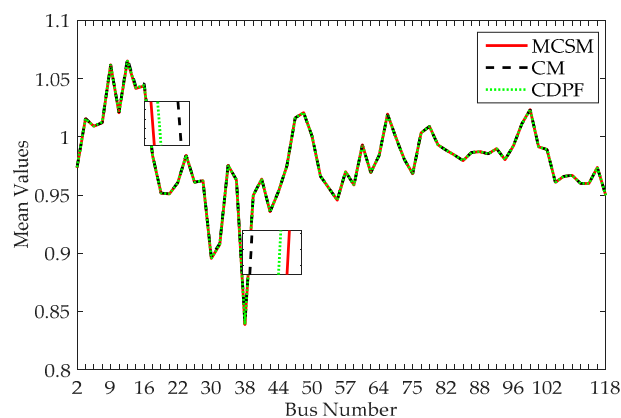


**Figure 13.** The means of the voltage magnitude at PQ buses in an IEEE 118-bus power system.

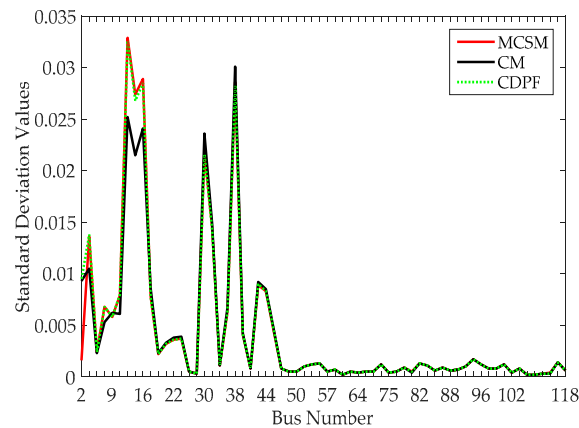


**Figure 14.** The Standard deviations of the bus voltage magnitude at PQ buses in an IEEE 118-bus power system.

**Table 5.** CPU time and calculation number  $N_{PL}$  of DPF.

MCSM		CM		CDPF	
$N_{PL}$	CPU Time (s)	$N_{PL}$	CPU Time (s)	$N_{PL}$	CPU Time (s)
10,000	526.2479	1	0.2052	513	71.2006

## 5. Conclusions

A novel PPF method considering continuous and discrete variables, called CDPF, is proposed in this paper. The mean, standard deviation, PDF, and CDF of power flow responses can be calculated accurately and efficiently by the proposed method. Continuous variables following a normal distribution or non-normal distribution and discrete variables following binomial distribution can be solved by the proposed method. The accuracy, efficiency, and applicability of the proposed method are demonstrated by comparing MCSM, CM and CDPF in IEEE 14-bus and IEEE 118-bus power systems. Conclusions are summarized as follows:

- (1) CDPF has better performance in computation speed compared with MCSM. Additionally, CDPF has a better performance in computation accuracy than CM, especially for the case with the large fluctuation range of input random variables.
- (2) CDPF has good performance in the applicability to deal with a discrete variable with different rated powers and multiple discrete variables in power systems.
- (3) CDPF has good performance in the applicability to address large power systems with high accuracy and efficiency.

In the future, the idea of the proposed method can be applied to other uncertainty analytical problems, such as the probabilistic static stability and the probabilistic reactive power control, and so on.

**Author Contributions:** Xuexia Zhang, Zhiqi Guo and Weirong Chen conceived this paper. Xuexia Zhang and Zhiqi Guo designed the experiments and analyzed the data. All authors wrote, reviewed and approved the manuscript.

**Conflicts of Interest:** The authors declare no conflict of interest.



## Glossary of Acronyms

PPF	probabilistic power flow
CM	cumulant method
MCSM	Monte Carlo simulation method
CDPF	power flow considering continuous and discrete variables
DPF	deterministic power flow
MDPF	multiple deterministic power flow
PDF	probability density function
CDF	cumulative density function
GCS	Gram-Charlier series
FCG	fuel cell generation
WPG	wind power generation
CPU	central processing unit

## References

1. Borkowska, B. Probabilistic load flow. *IEEE Trans. Power Appar. Syst.* **1974**, *3*, 752–759. [[CrossRef](#)]
2. Sun, Y.Y.; Mao, R.; Li, Z.Y.; Tian, W. Constant Jacobian matrix-based stochastic Galerkin method for probabilistic load flow. *Energies* **2016**, *9*, 153. [[CrossRef](#)]
3. Chen, Y.; Wen, J.Y.; Cheng, S.J. Probabilistic load flow method based on Nataf transformation and Latin hypercube sampling. *IEEE Trans. Sustain. Energy* **2013**, *4*, 294–301. [[CrossRef](#)]
4. Soleimanpour, N.; Mohammadi, M. Probabilistic load flow by using nonparametric density estimators. *IEEE Trans. Power Syst.* **2013**, *28*, 3747–3755. [[CrossRef](#)]
5. Zhang, S.X.; Cheng, H.Z.; Zhang, L.B.; Bazargan, M.; Yao, L.Z. Probabilistic evaluation of available load supply capability for distribution system. *IEEE Trans. Power Syst.* **2013**, *28*, 3215–3225. [[CrossRef](#)]
6. Zhang, H.; Li, P. Probabilistic analysis for optimal power flow under uncertainty. *IET Gener. Transm. Distrib.* **2010**, *4*, 553–561. [[CrossRef](#)]
7. Zou, B.; Xiao, Q. Solving Probabilistic optimal power flow problem using quasi Monte Carlo method and ninth-order polynomial normal transformation. *IEEE Trans. Power Syst.* **2014**, *29*, 300–306. [[CrossRef](#)]
8. Kaffashan, I.; Amraee, T. Probabilistic undervoltage load shedding using point estimate method. *IET Gener. Transm. Distrib.* **2015**, *9*, 2234–2244. [[CrossRef](#)]
9. Li, Y.M.; Li, W.Y.; Yan, W.; Yu, J.; Zhao, X. Probabilistic optimal power flow considering correlations of wind speeds following different distributions. *IEEE Trans. Power Syst.* **2014**, *29*, 1847–1854. [[CrossRef](#)]
10. Hong, Y.Y.; Lin, F.J.; Yu, T.H. Taguchi method-based probabilistic load flow studies considering uncertain renewables and loads. *IET Renew. Power Gener.* **2016**, *10*, 221–227. [[CrossRef](#)]
11. Rouhani, M.; Mohammadi, M.; Kargarian, A. Parzen window density estimator-based probabilistic power flow with correlated uncertainties. *IEEE Trans. Sustain. Energy* **2016**, *7*, 1170–1181. [[CrossRef](#)]
12. Villanueva, D.; Feijóo, A.E.; Pazos, J.L. An analytical method to solve the probabilistic load flow considering load demand correlation using the DC load flow. *Electr. Power Syst. Res.* **2014**, *110*, 1–8. [[CrossRef](#)]
13. Mohammadi, M. Probabilistic harmonic load flow using fast point estimate method. *IET Gener. Transm. Distrib.* **2015**, *9*, 1790–1799. [[CrossRef](#)]
14. Ren, Z.Y.; Li, W.Y.; Billinton, R.; Yan, W. Probabilistic power flow analysis based on the stochastic response surface method. *IEEE Trans. Power Syst.* **2016**, *31*, 2307–2315. [[CrossRef](#)]
15. Ruiz-Rodriguez, F.J.; Hernández, J.C.; Jurado, F. Probabilistic load flow for photovoltaic distributed generation using the cornish-fisher expansion. *Electr. Power Syst. Res.* **2012**, *89*, 129–138. [[CrossRef](#)]
16. Tamtum, A.; Schellenberg, A.; Rosehart, W.D. Enhancements to the cumulant method for probabilistic optimal power flow studies. *IEEE Trans. Power Syst.* **2009**, *24*, 1739–1746. [[CrossRef](#)]
17. Hajian, M.; Rosehart, W.D.; Zareipour, H. Probabilistic power flow by Monte Carlo simulation with Latin supercube sampling. *IEEE Trans. Power Syst.* **2013**, *28*, 1550–1559. [[CrossRef](#)]
18. Long, C.; Farrag, M.E.A.; Hepburn, D.M.; Zhou, C.K. Point estimate method for voltage unbalance evaluation in residential distribution networks with high penetration of small wind turbines. *Energies* **2014**, *7*, 7717–7731. [[CrossRef](#)]

19. Zhang, P.; Lee, S.T. Probabilistic load flow computation using the method of combined cumulants and Gram-Charlier expansion. *IEEE Trans. Power Syst.* **2004**, *19*, 676–682. [[CrossRef](#)]
20. Liu, J.; Hao, X.D.; Cheng, P.F.; Fang, W.L.; Niu, S.B. A parallel probabilistic load flow method considering nodal correlations. *Energies* **2016**, *9*, 1041. [[CrossRef](#)]
21. Bu, S.Q.; Du, W.; Wang, H.F.; Chen, Z.; Xiao, L.Y.; Li, H.F. Probabilistic analysis of small-signal stability of large-scale power systems as affected by penetration of wind generation. *IEEE Trans. Power Syst.* **2012**, *27*, 762–770. [[CrossRef](#)]
22. Fan, M.; Vittal, V.; Heydt, G.T.; Ayyanar, R. Probabilistic power flow analysis with generation dispatch including photovoltaic resources. *IEEE Trans. Power Syst.* **2013**, *28*, 1797–1805. [[CrossRef](#)]
23. Hong, Y.Y.; Lin, F.J.; Lin, Y.C.; Hsu, F.Y. Chaotic PSO-based VAR considering renewables using fast probabilistic power flow. *IEEE Trans. Power Deliv.* **2014**, *29*, 1666–1674. [[CrossRef](#)]
24. Sanabria, L.A.; Dillon, T.S. Stochastic power flow using cumulants and Von Mises functions. *Int. J. Electr. Power Energy Syst.* **1986**, *8*, 47–60. [[CrossRef](#)]
25. Hu, Z.C.; Wang, X.F. A probabilistic load flow method considering branch outages. *IEEE Trans. Power Syst.* **2006**, *21*, 507–514. [[CrossRef](#)]
26. Leite da Silva, A.M.; Arienti, V.L. Probabilistic load flow by a multilinear simulation algorithm. *Proc. Inst. Electr. Eng. C Gener. Transm. Distrib.* **1990**, *137*, 276–282. [[CrossRef](#)]
27. Li, Y.C.; Sun, G.Q.; Qian, X.R.; Shen, H.P.; Wei, Z.N.; Sun, Y.H. Probabilistic power flow calculation method of power system considering input variables with discrete distribution. *Power Syst. Technol.* **2015**, *39*, 3254–3259.
28. Wu, W.; Wang, K.Y.; Li, G.J.; Jiang, X.C.; Wang, Z.M. Probabilistic load flow calculation using cumulants and multiple integrals. *IET Gener. Transm. Distrib.* **2016**, *10*, 1703–1709. [[CrossRef](#)]
29. Cai, D.F.; Chen, J.F.; Shi, D.Y.; Duan, X.Z.; Li, H.J.; Yao, M.Q. Enhancements to the cumulant method for probabilistic load flow studies. In Proceedings of the 2012 IEEE Power and Energy Society General Meeting, San Diego, CA, USA, 22–26 July 2012.
30. Morales, J.M.; Perez-Ruiz, J. Point estimate schemes to solve the probabilistic power flow. *IEEE Trans. Power Syst.* **2007**, *22*, 1594–1601. [[CrossRef](#)]
31. Capitanescu, F.; Wehenkel, L. Sensitivity-based approaches for handling discrete variables in optimal power flow computations. *IEEE Trans. Power Syst.* **2010**, *25*, 1780–1789. [[CrossRef](#)]
32. Niknam, T.; Bornapour, M.; Gheisari, A. Combined heat, power and hydrogen production optimal planning of fuel cell power plants in distribution networks. *Energy Convers. Manag.* **2013**, *66*, 11–25. [[CrossRef](#)]
33. Fan, M.; Vittal, V.; Heydt, G.T.; Ayyanar, R. Probabilistic power flow studies for transmission systems with photovoltaic generation using cumulants. *IEEE Trans. Power Syst.* **2012**, *27*, 2251–2261. [[CrossRef](#)]
34. Ruiz-Rodriguez, F.J.; Hernandez, J.C.; Jurado, F. Probabilistic load flow for radial distribution networks with photovoltaic generators. *IET Renew. Power Gener.* **2012**, *6*, 110–121. [[CrossRef](#)]
35. Williams, T.; Crawford, C. Probabilistic load flow modeling comparing maximum entropy and Gram-Charlier probability density function reconstructions. *IEEE Trans. Power Syst.* **2013**, *28*, 272–280. [[CrossRef](#)]

